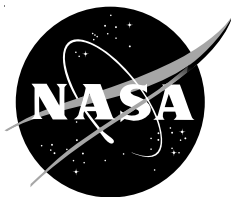# Pegasus® Wing-Glove Experiment to Document Hypersonic Crossflow Transition—Measurement System and Selected Flight Results

Arild Bertelrud
Analytical Services and Materials, Inc.
Edwards, California

Geva de la Tova
Computer Sciences Corporation
Edwards, California

Philip J. Hamory, Ronald Young, Gregory K. Noffz, and Michael Dodson
NASA Dryden Flight Research Center
Edwards, California

Sharon S. Graves, John K. Diamond, and James E. Bartlett
NASA Langley Research Center
Hampton, Virginia

Robert Noack
WYLE Laboratories
Hampton, Virginia

David Knoblock
NASA Kennedy Space Center
Cape Canaveral, Florida

January 2000

The NASA STI Program Office...in Profile

Since its founding, NASA has been dedicated to the advancement of aeronautics and space science. The NASA Scientific and Technical Information (STI) Program Office plays a key part in helping NASA maintain this important role.

The NASA STI Program Office is operated by Langley Research Center, the lead center for NASA's scientific and technical information. The NASA STI Program Office provides access to the NASA STI Database, the largest collection of aeronautical and space science STI in the world. The Program Office is also NASA's institutional mechanism for disseminating the results of its research and development activities. These results are published by NASA in the NASA STI Report Series, which includes the following report types:

- TECHNICAL PUBLICATION. Reports of completed research or a major significant phase of research that present the results of NASA programs and include extensive data or theoretical analysis. Includes compilations of significant scientific and technical data and information deemed to be of continuing reference value. NASA's counterpart of peer-reviewed formal professional papers but has less stringent limitations on manuscript length and extent of graphic presentations.

- TECHNICAL MEMORANDUM. Scientific and technical findings that are preliminary or of specialized interest, e.g., quick release reports, working papers, and bibliographies that contain minimal annotation. Does not contain extensive analysis.

- CONTRACTOR REPORT. Scientific and technical findings by NASA-sponsored contractors and grantees.

- CONFERENCE PUBLICATION. Collected papers from scientific and technical conferences, symposia, seminars, or other meetings sponsored or cosponsored by NASA.

- SPECIAL PUBLICATION. Scientific, technical, or historical information from NASA programs, projects, and mission, often concerned with subjects having substantial public interest.

- TECHNICAL TRANSLATION. English-language translations of foreign scientific and technical material pertinent to NASA's mission.

Specialized services that complement the STI Program Office's diverse offerings include creating custom thesauri, building customized databases, organizing and publishing research results...even providing videos.

For more information about the NASA STI Program Office, see the following:

- Access the NASA STI Program Home Page at *http://www.sti.nasa.gov*

- E-mail your question via the Internet to help@sti.nasa.gov

- Fax your question to the NASA Access Help Desk at (301) 621-0134

- Telephone the NASA Access Help Desk at (301) 621-0390

- Write to:
  NASA Access Help Desk
  NASA Center for AeroSpace Information
  7121 Standard Drive
  Hanover, MD 21076-1320

NASA/TM-2000-209016
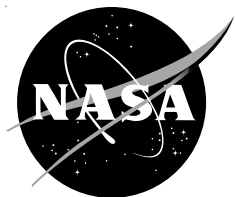
Pegasus® Wing-Glove Experiment to Document Hypersonic Crossflow Transition—Measurement System and Selected Flight Results

Arild Bertelrud
Analytical Services and Materials, Inc.
Edwards, California

Geva de la Tova
Computer Sciences Corporation
Edwards, California

Philip J. Hamory, Ronald Young, Gregory K. Noffz, and Michael Dodson
NASA Dryden Flight Research Center
Edwards, California

Sharon S. Graves, John K. Diamond, and James E. Bartlett
NASA Langley Research Center
Hampton, Virginia

Robert Noack
WYLE Laboratories
Hampton, Virginia

David Knoblock
NASA Kennedy Space Center
Cape Canaveral, Florida

National Aeronautics and
Space Administration

Dryden Flight Research Center
Edwards, California 93523-0273

January 2000

Available from the following:

PEGASUS® WING-GLOVE EXPERIMENT TO DOCUMENT HYPERSONIC CROSSFLOW TRANSITION—MEASUREMENT SYSTEM AND SELECTED FLIGHT RESULTS

Arild Bertelrud[*]
Analytical Services and Materials, Inc.
Edwards, California

Geva de la Tova[†]
Computer Sciences Corporation
Edwards, California

Philip J. Hamory,[‡] Ronald Young,[§] Gregory K. Noffz,[¶] and Michael Dodson[**]
NASA Dryden Flight Research Center
Edwards, California

Sharon S. Graves,[††] John K. Diamond,[‡‡] and James E. Bartlett[§§]
NASA Langley Research Center
Hampton, Virginia

Robert Noack[¶¶]
WYLE Laboratories
Hampton, Virginia

David Knoblock[***]
NASA Kennedy Space Center
Cape Canaveral, Florida

Abstract

In a recent flight experiment to study hypersonic crossflow transition, boundary layer characteristics were documented. A smooth steel glove was mounted on the first stage delta wing of Orbital Sciences Corporation's Pegasus® launch vehicle and was flown at speeds of up to Mach 8 and altitudes of up to 250,000 ft. The wing-glove experiment was flown as a secondary payload off the coast of Florida in October 1998. This paper describes the measurement system developed. Samples of the results obtained for different parts of the trajectory are included to show the characteristics and quality of the data. Thermocouples and pressure sensors (including Preston tubes, Stanton tubes, and a 'probeless' pressure rake showing boundary layer profiles) measured the time-averaged flow. Surface hot-films and high-frequency pressure transducers measured flow dynamics. Because the vehicle was not recoverable, it was necessary to design a system for real-time onboard processing and transmission. Onboard processing included spectral averaging. The quality and consistency of data obtained was good and met the experiment requirements.

[*] Aerospace Engineer, Member AIAA
[†] Instrumentation Engineer
[‡] Instrumentation Engineer
[§] Instrumentation Engineer
[¶] Aerospace Engineer
[**] Flight Assurance Analyst
[††] Aerospace Engineer
[‡‡] Instrumentation Engineer
[§§] Instrumentation Engineer
[¶¶] Engineering Technician
[***] Software Specialist

Nomenclature

AC	alternating current
DAPS	Data Acquisition and Processing System

dB	decibels
DC	direct current
FTF	flight test fixture
g	gravity
kHz	kilohertz
M	Mach number
Mbit/sec	Megabits per second
ms	millisecond
mV	millivolts
NASA	National Aeronautics and Space Administration
OSC	Orbital Sciences Corporation, Dulles, Virginia
PCM	pulse code modulation
PHYSX	Pegasus Hypersonic Experiments
PSD	power spectral density
psi	pounds per square inch
Re	Reynolds number
RMS	root-mean-square
sps	samples per second
t	time
TC	thermocouple
V	volts

Introduction

Interest in air-breathing flight at hypersonic speed has prompted research to improve the understanding of aerodynamic and aerothermodynamic flow phenomena over hypersonic vehicles. The understanding of transition from laminar to turbulent flow is of both fundamental and practical importance, because the onset of transition dictates the forebody boundary-layer thickness entering the inlet. It also affects local heating which is a critical element in the design of hypersonic vehicles.

In order to validate transition codes at Mach numbers and Reynolds numbers commensurate with future hypersonic air-breathing vehicles, a series of flight experiments aboard the Orbital Sciences Corporation (OSC), (Dulles, Virginia) Pegasus® launch vehicle were defined. These experiments, called PHYSX (Pegasus HYperSonic eXperiments), incrementally led to the identification of important transition characteristics at Mach numbers from 5 to 8 and altitudes above 100,000 ft. References 1 and 2 describe the plans for and the development of these experiments.

In 1994 the FX-A experiment was flown to examine important measurement issues, and in 1998 the FX-1 experiment was flown using an instrumented wing glove. This paper focuses on the essential features of the measurement system and data processing techniques used in the latter experiment. Selected flight results are included in order to illustrate the quality of the data. A detailed analysis of the data will be reported separately.

Note that use of trade names or names of manufacturers in this document does not constitute an official endorsement of such products or manufacturers, either expressed or implied, by the National Aeronautics and Space Administration.

Requirements

To carry out this experiment certain requirements were imposed. The aerodynamics and structure of the glove, measurement parameters, signal processing needs, and operational limitations all had to be accommodated.

Aerodynamic and Glove Requirements

In aerodynamic flight research it is often beneficial to conduct studies with a 'glove,' i.e. a geometrical shape mounted to a wing, external to the existing structure. To study the characteristics of crossflow transition, FX-1 required a glove that amplified crossflow disturbances and dampened out Tollmien-Schlichting disturbances.

For laminar and transitional flow over the glove, the attachment-line boundary layer needed to be laminar. As a rule of thumb, this means that the Reynolds number needed to be below 100,000 based on the radius of curvature at the attachment line. Furthermore, the angle of attack had to be small in order to obtain the required pressure distribution.

Any discontinuity in the radius of curvature of the glove or of the vehicle-glove fairing inboard and upstream of the glove could cause a shock. The glove had to be smooth and free of waviness. The roughness criterion states that the Reynolds number should be smaller than 10 based on local free-stream velocity and roughness height.[3] Acceptable waviness is on the order of 0.0002.[4]

The fairing had to be nonablative in order to preclude contamination in the flow over the glove. To support design choices (enumerated in the Instrumentation section of this paper), the glove surface had to be thermally conductive and thin.

The glove also had to be strong enough to take the loads experienced as the vehicle accelerates to supersonic speeds at an 18° angle of attack, and it had to be installed with minimum modification to the existing wing structure and with no significant change to the wing stresses.

Measurement Requirements

Since this was a code validation experiment, the parameters modeled in the codes were the required measurements. Those code parameters were transition location, fluctuation intensity, disturbance frequencies, and propagation speed and direction. Boundary conditions consisted of temperature distributions, surface pressure distribution, boundary layer profile, and flow direction. Mach number, Reynolds number, angle of attack, free-stream turbulence characteristics and vibration level measurements were also needed.

The most important parameters were measured either with more than one technique or with multiple uses of the same technique. There were three reasons for this. The first reason was operational. The wing-glove would fly only once, and because there was no guarantee that repairs could be made to failed sensors or signal conditioning, measurement redundancy was required in order to minimize the risk of not meeting these requirements. Secondly, when independent techniques are used, uncertainties in the results from one technique can be reduced by having the results of another technique. For example, if heat flux and pressure changes result from the passage of transition, detecting both of those changes can clarify where and when transition did in fact begin and end. Finally, multiple measurements make it possible to systematically evaluate the effect of certain unknowns. For example, if it is not clear in advance what interference the physical size of a sensor might have on the measurement, two sensors of different size can be used and their results can be compared.

Proven measurement techniques were used. However, when none existed or when a proven technique was used in a new way or in a way that exceeded previous experience with that technique, laboratory testing (and, if necessary, precursor flight testing) was done to establish confidence in the technique.

It was also necessary to assume that any external sensor or instrumentation would cause transition. Thus any instrumentation protruding above the glove surface was required to be toward the rear of the glove. Furthermore, computed wall streamlines were required in lieu of pressure ports in the leading edge region, because disturbances resulting from those ports would spread to the main portion of the glove.

Signal Processing Requirements

Power spectral densities (PSD), correlations in time and space, and statistics were required in order to document the physics of the transition process as completely as possible. For these analyses to be effective, the frequency content of the data needed to be high, up to 25 kHz.

Ideally, every time-series sample contributing to these analyses would be recorded. However, the total data rate required for doing so would have been 10 Megabits per second (Mbit/sec). Three operational limitations made recording all the data impossible: (1) the maximum real-time telemetry data rate available was 0.8 Mbit/sec; (2) the data could not be recorded onboard the vehicle and processed postflight because the Pegasus® was not to be recovered; (3) the data could not be buffered onboard the vehicle and transmitted at a lower rate before the end of the flight because of the short flight time.

Because of these limitations, the requirement emerged for onboard signal processing equipment that could acquire data at a 10 Mbit/sec rate and then process the data in some way that would fit the required content into a 0.8 Mbit/sec telemetry link. The equipment would either need to (1) pass on enough data for meaningful PSDs, correlations, and statistics to be computed on the ground, or (2) it would need to perform the analyses in real-time and transmit the results, or (3) it would need to do a combination of (1) and (2). Since transition physics change appreciably as Mach number increases, any real-time analysis would need to be accomplished within the time that Mach number changes by 0.01; that is, within 100 milliseconds (ms).

Operational Requirements

FX-1 was planned as a secondary payload aboard the Pegasus® because the experiment objectives could be met without going to the expense of purchasing a dedicated launch. As a result of being a secondary payload, however, FX-1 had to be integrated into a launch with the minimum possible schedule impact. This meant that FX-1 hardware needed to be assembled

independently (as much as possible) from the rest of the vehicle. It also meant that there might not be any opportunities to repair failed sensors or signal conditioning after integration with the primary payload.

Initially, there was no requirement for real-time control room displays during the launch or during the captive-carry flight leading to launch. The only reason to have such displays would be to have the ability to notice system failures and repair them before launch. The option to repair was not going to be available to FX-1 since it was a secondary payload. However, as the investment in FX-1 grew with time, real-time displays and the option to repair critical systems became requirements. Since the cost of delaying a launch would grow as the launch grew nearer, the requirement for decision-tree analysis was added. The decision tree would systematically organize the research objectives, the relevant instrumentation, the potential failure modes of that instrumentation, and the factors involved in repairing that instrumentation so that the FX-1 project manager could know in advance what decision to make (to delay or not to delay) in the event of system failures.

Vehicle Description, Trajectory, and Flow Field

The Pegasus® is a three-stage solid-rocket launch vehicle,[5] designed for launch from a carrier airplane (currently an L-1011) at Mach 0.8 and an altitude of 40,000 ft. The first stage of the Pegasus® has a delta wing with a leading-edge sweep of 45°. Figure 1 illustrates the geometry of the Pegasus® with the glove and its fairing on the starboard wing. The vehicle consists of a blunt-nosed cylindrical body of 50 in. (1.27 m) in diameter and 50 ft (15.24 m) in length. Except for the glove and the ceramic-tile fairing, the vehicle is coated with an ablative for thermal protection.

Figure 2 illustrates how the Pegasus® is launched from the L-1011 and how the payload is put into orbit. Only the first-stage flight was relevant to the experiment since the glove was part of Stage 1.

The time histories of Mach number, altitude, and angle of attack in Figure 3 illustrate the trajectory as a function of time. The vehicle is dropped from the L-1011 at time 0. The engine fires at time = 5 sec. Then the vehicle goes through Mach 1 and pitches up to an 18° angle of attack. With the lift provided by the delta wing, the vehicle begins to gain altitude. The main flight regime of interest for FX-1 is the portion of the trajectory where the angle of attack has been reduced almost to zero and the attachment line is laminar.

The trajectory may also be expressed in other parameters related to flow conditions and instrumentation. Figure 4 has unit Reynolds number and ambient and dynamic pressures plotted against Mach number. The figure illustrates how the pressures change by almost three orders of magnitude during the first-stage flight. This has consequences for the measurement resolution of the 12-bit data acquisition system. Adaptive gain was not used for reliability and bookkeeping reasons. Instead, the gains were set to large values and signal saturation in the first portion of the flight was accepted.

The vehicle flow field is governed by two shocks: the bow shock and the wing shock; i.e. the disturbance field of the transitional flow is processed through two shocks. Also, the pressure is higher than ambient and the local Mach number is lower. The wall temperature on the glove is always lower than the adiabatic wall temperature.

The flow around the vehicle in general, and around the glove in particular, was computed extensively using Navier-Stokes codes, Euler codes, and boundary layer codes. Since the trajectory was known only in general terms, the sensitivity of disturbance amplification with respect to reference condition was explored systematically through computations involving the potential range of angle of attack, Mach number, Reynolds number, and wall temperature.[6]

Glove Engineering and Design

To limit the changes to the vehicle, the experiment was conducted using a part-span glove mounted on the starboard side, with an appropriate counterweight on the port side. Figure 5 is a photograph of the glove mounted on the wing. Figure 6 is a plan view showing detail of the glove and fairing.

In order to design a glove that could handle the thermal and structural loads, it was necessary to examine the trajectory in terms of local heat loads. The heat transfer analysis was performed using two different assumptions: an initial laminar and an initial turbulent attachment line at the leading edge with an appropriate transition criterion for the upper skin surface of the glove.[7]

The glove was made out of steel. A solid leading-edge structure (fig. 7) was used as a heat sink, but the rest of the glove had a thin skin as required. The thin skin also

made the thermal stress throughout the test surface relatively uniform. In order to meet the smoothness requirements, special care was taken between the inboard glove leading edge, the fairing, and the original wing surface. The glove was rigidly attached to the wing only at the inboard leading edge in order to account for differential expansion of the glove and wing during flight. The glove could expand parallel to the leading edge and back from the leading edge without adding mechanical stresses.

The substructure of the glove was made of end-grain balsa wood smoothly contoured to the inner shape of the thin skin of the glove. The skin was held tightly against this balsa surface (but was free to slide) by 270 spring attachments through swivel studs bonded to the steel.[8] The glove surface was hand finished and nickel-plated for corrosion protection.

A complete ground-test glove was manufactured and tested in the NASA Dryden Flight Loads Laboratory. The ground-test glove was mounted on a mock-up wing and exposed to the thermal loads anticipated for the flight glove. The thermal loads prescribed in the ground test were determined using a transient, three-dimensional finite-element analysis.[7] The instrumentation used in the ground test included thermocouples, strain gages, and heat flux sensors. Details of the thermal ground test are provided in references 9 and 10.

Operational Aspects

The first stage of the Pegasus® vehicle consists of a fuselage, a wing, and a wing/fuselage fillet. These parts were assembled and integrated with the second and third stages of the vehicle a short time (weeks) before launch. In order to meet the requirement for FX-1 to be assembled independently from the rest of the vehicle, FX-1 hardware was limited to installation on or in the wing and the wing/fuselage fillet. With a wing and a fillet provided by OSC, NASA was able to mount the glove, fairing, and instrumentation and could check the functionality of the instrumentation without being tied directly to a particular launch. This task was completed during the fall of 1996.

The FX-1 wing and fillet was integrated with the rest of the vehicle at Vandenberg Air Force Base, California, during the summer of 1998 when a primary payload with a suitable trajectory and adequate weight margin was identified. Final instrumentation integration and calibrations were performed at this time. Final wing surface quality and geometry inspection and documentation was performed there as well and

compared with previous inspections at NASA and at the OSC Chandler, Arizona, facility.

The Pegasus® was ferried to Cape Canaveral Air Station, Florida, where launch operations took place. Real-time control room displays had been developed for monitoring all essential FX-1 parameters. The decision tree had made clear what backup instrumentation was necessary to have on hand and what courses of action would be taken depending on what failures occurred and when they occurred. The displays and the decision tree proved to be invaluable tools.

Instrumentation

FX-1 instrumentation was divided up conceptually into low-frequency and high-frequency instrumentation. The low-frequency instrumentation was sampled at 300 samples per second (sps) or less and provided time-averaged observations of transition location, surface pressure distribution, boundary layer profile, flow direction, and vehicle body motion. High-frequency instrumentation was used to identify frequencies, wavelengths, and propagation speed and direction of turbulence in order to determine the reasons for changes in the time-averaged observations. High-frequency instrumentation was also used to obtain free-stream turbulence and glove vibration level.

The remainder of the required measurements (Mach number, Reynolds number, and angle of attack) was obtained independently from three sources: (1) the Pegasus® telemetry system (which included an inertial navigation system and a global positioning system); (2) ground-based radar tracking facilities; and (3) weather balloons and meterological rockets launched before and after the Pegasus® launch as close in time as was safely possible.

The onboard instrumentation made additional measurements that are not discussed in this paper (because they are not related to the measurement requirements for the boundary layer transition experiment). Those measurements were temperature of the ceramic fairing tiles, glove strain, and power supply and excitation voltages.

Low-Frequency Instrumentation

A proven technique for detecting transition is to measure local temperature development and heat transfer.[11, 12] Type K foil thermocouples (TCs) were mounted immediately underneath the surface of the glove, this is the reason the glove surface had to be thermally conductive. Inboard, center, and outboard

American Institute of Aeronautics and Astronautics

rows of 20 to 24 TCs each were used; between those rows were two additional rows of four to five TCs each. Time histories from these thermocouples went into a one-dimensional inverse heat transfer analysis[13] and a backwards finite difference computing technique.[11] Both analyses allow an estimate of true surface temperature and heat flux. The requirement that the glove surface be thin came from these analyses. Electronic cold junction compensation was used for the TCs.

A row of five Stanton tubes[14] with a Preston tube[15] at each end and with local static pressure reference ports was installed spanwise across the glove toward the rear edge of the upper surface. These instruments were to gather additional information on the passage of transition. The total pressure changes drastically as transition moves past the tubes, and the spanwise measurements yield information on possible turbulent wedges occurring along the span of the glove.

The surface pressure distribution was measured with two rows of pressure ports, one inboard row having 32 ports and one outboard row having 40 ports. Computed wall streamlines were used in lieu of ports in the leading edge region of the inboard row since a disturbance from these ports would have spread to the main portion of the glove. Each pressure port was 0.0625 inches in diameter.

Traditionally, rakes with total pressure tubes are used to document the boundary layer shape. However, because the heat loads on such a rake would have been too high during this experiment, two 'probeless' rakes, based on the concepts of Keener and Hopkins,[16] were used. The FX-1 rakes were 6-degree half-angle wedges with blunt leading edges and flat sides (fig. 8). The taller rake had eight total pressure ports drilled in the face, and the highest port was 2 inches above the glove surface. Two ports were drilled in the face of the shorter rake. Both rakes also had a pressure port on each side. Two rakes rather than one were used in order to have additional measurements close to the glove surface and to have data that could be used to evaluate the effect of probe height on the measurement.

Tests were conducted in a hypersonic Helium-flow wind tunnel to compare the performance of the taller probeless rake with a traditional rake. These tests showed that Mach number had to be greater than 2 for the total pressure readings to provide valid information; readings from the ports in the subsonic part of the boundary layer were identical. These results are consistent with a theoretical calibration based on the Rayleigh Pitot tube formula.[17]

Readings from the side ports, however, were valid at all Mach numbers and could be used to determine approximate flow direction when the shock (for flow greater than Mach 1) was attached. The higher the Mach number, the larger the angle that could be determined.

Absolute pressure was measured through a reference tank using a 20-bit thermally compensated transducer. All other low-frequency pressures were measured by electronically scanned differential pressure modules referenced to the tank through pneumatic tubing of equal length, so that the time lag of all the pressure ports would be equal. The temperature of the differential modules was actively controlled, and the reference tank was free to vent as the flight progressed.

The full-scale range of the differential pressure transducers measuring the rake and Preston tube total pressures was ± 10 pounds per square inch (psi). The full-scale range for all other low-frequency differential pressure measurements was ± 5 psi to provide sufficient resolution in the low-pressure experiment window (late in the flight). Thus, because of the three-order-of-magnitude change in pressure anticipated during flight (see fig. 4), the ± 5 psi transducers were overpressured during the high-pressure portion of the flight (early in the flight). Because overpressure was expected, those transducers were tested to ± 8 psi prior to flight, and a comparison of the calibrations before and after the test showed that overpressuring the transducers did not cause a change to the calibration.

A ± 10-g three-axis accelerometer package was also used. It was located near the Stage 1 center of gravity and was used to measure vehicle body motion.

High-Frequency Instrumentation

Hot-film anemometry and the measurement of local pressure fluctuations are two proven techniques for identifying the frequencies, wavelengths, and propagation speed and direction of disturbances.[18] A dual hot-film sensor usable in high temperatures was developed specifically for FX-1.[19] The sensor had two orthogonal pairs of nickel thin-films deposited on a 0.5 in. diameter cured silica plug (fig. 9) that was flush-mounted into the glove surface. Each pair of films consisted of an active element (the hot film) and a passive element (for sensing ambient temperature). The films were operated by temperature-compensated anemometry[20] that maintained the hot films at an overheat ratio of 1.3 with respect to ambient temperature. Three of these dual sensors were installed toward the rear of the glove (fig. 8). Precursor flight

testing (discussed in that section of the paper) was used to establish confidence in the sensor design.

An array of three high-frequency differential pressure transducers was installed near the dual hot-film sensors and was used to measure the local pressure fluctuations (fig. 8). Signal conditioning was set for full-scale readings of approximately 0.1 psi (150 dB sound pressure level). Because the sensing area of these transducers was too large and the sensing surface was too rough to be mounted flush with the glove surface, the transducers were mounted under the glove surface beneath pinholes.

It was not the steady-state level of pressure but the high-frequency fluctuations in pressure that were of interest for this measurement, so any convenient volume of air large enough to serve as a low-pass filter was adequate for the reference port of these transducers. Therefore, the reference port was open to the inside of the glove. This volume vented freely during the flight.

Although high-frequency pressure transducers had been used in previous transition flight experiments,[21] some laboratory work was required to refine the amplitude and phase relations between the would-be flush-mounted transducers and the actual pinhole-mounted transducers. The test apparatus assembled for this purpose consisted of a loudspeaker and a funnel for guiding the sound waves down to the transducer. The bottom of the funnel adapter represents the glove surface. Figure 10 parts (a) and (b) show two test configurations: one with a flush-mounted transducer and one with a pinhole-mounted transducer. In the side wall of the neck of the funnel, a reference transducer was mounted and adjusted until the amplitude and phase of its signal matched those of the signal obtained with the flush-mounted transducer (fig. 10(a)). In this way, the amplitude and phase differences obtained between the flush-mounted transducer and the pinhole-mounted transducer would be determined when the configuration in (fig. 10(b)) was used. Figure 10(c) is a photograph of the actual hardware. White noise was the stimulus for the calibration. Calibrations were performed both at sea level pressure and in a vacuum chamber set to pressures corresponding to altitudes of 60,000, 70,000, and 80,000 ft. 80,000 ft was as high as the test equipment would operate.

It is worth noting that pinhole mounting made it possible to use a transducer with a standard temperature range (–65 °F to 250 °F) rather than a high temperature range (–65 °F to 500 °F). It is also worth mentioning that prior to the selection of the pinhole-mounted approach for making this measurement, the use of graphite as an ablator for these transducers was tested as a means for protecting the transducers from high temperatures. That approach, however, was not pursued further because of the uncertain effect of ablation on calibration.

Free-stream fluctuations were also measured with a high-frequency differential pressure transducer whose signal conditioning was set for full-scale readings of approximately 0.1 psi (150 dB sound pressure level). The transducer was mounted forward-facing above the surface of the glove in a metal housing shown in figure 8. This transducer also had a standard temperature range and depended on the heat-sinking capability of the housing to keep it within range.

Glove vibrations were measured with accelerometers. The root-mean-square (RMS) signal levels of these accelerometers were set to 5-g RMS full-scale.

Figure 11 illustrates the sensor layout. It also depicts an example transition scenario.

Data Acquisition System

The data acquisition system was located in the wing/fuselage fillet of the Pegasus. Low-frequency instrumentation was connected to a 12-bit pulse code modulation (PCM) system through analog signal conditioning electronics. High-frequency instrumentation was connected to the PCM system by one or more onboard signal processing systems described in the next section. The total bit rate was 0.8 Mbit/sec.

Onboard Signal Processing

Three types of onboard signal processing systems were used for FX-1. The primary system was called the Data Acquisition and Processing System (DAPS).[22] Two of these four-channel systems were used: one for acquiring data from two of the dual hot-film sensors and the other for acquiring data from the four high-frequency pressure transducers. Each DAPS channel acquired information for up to 25 kHz by sampling at 100,000 sps. For eight channels, the total acquisition rate was 9.6 Mbit/sec.

The approach selected for meeting the requirement of fitting nearly 10 Mbit/sec of data into a 0.8 Mbit/sec telemetry link was to compute the PSDs and selected statistics in real-time, onboard the vehicle, and pass them on with enough time-series data so that the

correlations and the remainder of the statistics could be computed on the ground postflight. The following paragraphs explain the rationale for this approach.

The first consideration is the volume of the data that PSDs, correlations, and statistical analyses produce. Correlations expand the volume of data to the extent that computing those onboard the vehicle would have been counterproductive. On the other hand, spectral analysis often involves the ensemble averaging of PSDs. Averaging reduces the volume of data. Likewise, statistical moments also reduce the volume of data. Therefore, it made sense to summarize the data that could not be downlinked into ensemble-averaged PSDs and selected statistics (mean and standard deviation).

The second consideration is related to the requirement that real-time analyses be accomplished within the time that Mach number changes by 0.01; that is, within 100 ms. The assumption behind this requirement is that the boundary layer is stationary, statistically speaking, during this time. If this assumption is true, then an analysis over any sufficiently long subset of the 100 ms would reveal the same characteristics that an analysis over the whole 100 ms would reveal. The only exception to that statement would be that the shorter analysis would have lower resolution than the analysis over the whole 100 ms, because fewer data points are used.

The third consideration is resolution. Since the PSDs, statistics, and time-series data all have to fit in the same 0.8 Mbit/sec link, the more resolution given to the ensemble-averaged PSDs, the less time-series data that can be downlinked. Likewise, the more time-series data downlinked, the lower the resolution in the PSDs. For the following reasons, the decision was made to use 512-point time-series records and 512-point PSDs: (1) 512 points covered satisfactorily the time scale of interest for the correlations; (2) 512 points at 100,000 sps yields a satisfactory frequency resolution of approximately 200 Hz; (3) 512-point records made each downlinked PSD the ensemble average of a satisfactory number of records, namely 20 records; (4) using the same number of points makes it easy to compare a PSD-generated postflight from the time-series data with the downlinked PSD. The two PSDs would be similar if the signal was stationary.

The time-series record that was downlinked covered only 5 ms of the 100 ms flight condition. In order to determine how well these 5 ms of data represent the whole 100 ms, the following computations and comparisons were performed. DAPS computed the standard deviation of each 512-point time-series record that went into the ensemble-averaged PSD. For those records, DAPS noted and relayed the minimum, average, and maximum standard deviations. These statistics provided an indication of the consistency between each 5 ms subset of the 100 ms flight condition. Likewise, the standard deviation of the one downlinked time-series record would be compared to those statistics to determine how well the record represented the whole 100 ms. Finally, the PSD comparison mentioned at the end of the previous paragraph would also provide an indication of how well the record represented the whole 100 ms.

Note that although the PSDs had 512 points, only the first 151 points representing frequencies up to 29 kHz were downlinked. The first 128 points representing frequencies up to 25 kHz would have been adequate, but the structure of the PCM downlink made it convenient to transmit the extra points. In contrast, the structure of the PCM downlink limited the downlinked time-series to only 498 points instead of 512 points. Although less than ideal, 498 was close enough to 512 to satisfy the rationale stated earlier for the 512-point time-series records. DAPS also computed and relayed the number of zero crossings for each 100 ms and transmitted frame counting and synchronization information.

In addition to DAPS, two other types of onboard signal processing systems were used. One was a four-channel swept-tuned spectrum analyzer[23] which provided information up to 25 kHz for two of the hot-films and two of the high-frequency pressure transducers. This 'sweep analyzer' had been used on FX-A and was used on FX-1 mainly as a backup in the event either four-channel DAPS failed. The other type of signal processing system was a wideband RMS system. This system was used for monitoring signal level and for crude characterization of the hot-film, high-frequency pressure, and vibration signals. It converted the true RMS values of these high-frequency signals to DC levels over a 100 ms averaging time and passed the result to the PCM system.

Figure 12 is a pictorial summary of the onboard instrumentation and signal processing used for FX-1. It shows the low- and high-frequency sensors and their connections to the PCM system through signal conditioning or through signal processing.

Precursor Flight Testing

Two flight experiments were conducted in order to develop the PHYSX instrumentation approach. The purpose for an experiment flown in June 1994 on the

Pegasus[®] Step-1 (FX-A) launch was to determine the vibration environment in the wing/fuselage area resulting from rocket burn to verify that the selected sensors and the sweep analyzer would tolerate the environment and provide useful data. A panel in the wing/fuselage fillet had been instrumented with surface hot-films, high-frequency pressure transducers and pressure ports of varying diameter and line lengths to resolve pressure lag issues for the ports in the wing glove. Accelerometer data showed that the majority of the vibrations were limited to roughly 4 kHz and that the maximum amplitude was reached roughly 20 seconds after launch.[24]

While the FX-A launch provided data for turbulent flow on the sidewall panel, the flight tests with the NASA Dryden F-15 Flight Test Fixture (FTF) provided data in a transitional flow.[2] The experiment served to verify both the functionality of the high-frequency sensors in a transitional environment and the ability of the DAPS to characterize that transitional flow.

An array of sensors was mounted on the elliptical nose of the FTF, both to determine the transition location as a function of flight condition and to examine its characteristics. Thus the effect of a transition front sweeping past a sensor array, as anticipated for FX-1, could be examined. It was demonstrated that transition passage could be detected by the low-frequency measurements (Preston tubes, Stanton tubes, and hot-film DC level), while spectra from both hot-film and high-frequency pressure transducers were needed for a positive identification of the cause of transition.

Results

In this section some examples of results obtained from FX-1 are presented. Transition, turbulent and laminar flow, boundary layer profile, pressure distributions, vibrations and staging are discussed.

Transition

Figure 13 shows the time history of one thermocouple before and after transition passes the sensor. Because the transition region moves aft on the glove surface as time progresses (as the unit Reynolds number decreases), the sensor is exposed to a turbulent boundary layer first and then to a laminar boundary layer. The difference in slope clearly shows the change from turbulent flow to laminar flow. This figure illustrates the value of having abundant samples even for a low-frequency measurement.

Figure 14(a) shows the time histories from a dual hot-film sensor during transition. Figure 14(b) shows the time history from one of the surface high frequency pressure transducers during transition. The upward spikes in figure 14(a) show that the flow is mostly laminar and contains turbulent spikes. The downward spikes in figure 14(b) show that the flow is mostly turbulent and contains laminar spikes.

Figure 15 shows the flatness (*kurtosis*) computed from the DAPS time-series data for both hot-films of a dual hot-film sensor. Both hot-film signals exhibit peaks in the measure of flatness, a feature that is consistent with transition.[25] Meanwhile, lack of change in the flatness of the free-stream turbulence measurement obtained by the forward-facing high-frequency pressure transducer indicates that the transducer was indeed outside the boundary layer.

It is worth noting that the flatness computed from the DAPS time-series data for the three surface high-frequency pressure transducers also contained peaks in the measure of flatness.

Turbulent and Laminar Flow

Bridge voltage readings for one hot-film in both turbulent and laminar flow are shown in figure 16. The steady-state signal is the set of low sample-rate readings. The RMS signal is the output of the wideband RMS system for the measurement. The higher levels for both signals indicate turbulence and the lower levels indicate laminar flow.

Figure 17 shows time histories of standard deviation or RMS for one hot-film signal passed through three processing techniques. One curve was produced by the wideband RMS system. The second curve was the average standard deviation produced by the DAPS unit. The individual points are the standard deviations computed postflight from selected 498-point DAPS time series. The individual points are consistent with the results obtained by onboard processing. The larger readings are for turbulent flow, and overall, the slow variation of the standard deviation confirms the turbulent nature of the flow during this time period. Results from mostly laminar readings are shown for comparison.

Boundary Layer Profile

The probeless rake data confirmed the previous assessments that the Mach number had to be greater than 2 for the rake to provide valid information. In the

subsonic part of the boundary layer, the ports gave the same value. Figure 18 shows examples of Mach number distribution for three flight Mach numbers where the data is valid. The curves indicate boundary layer thicknesses slightly above 1 in., and the laminar case exhibits rake-induced separation.

As mentioned previously, the rakes also provided information on the crossflow angle. Figure 19 shows the indicated crossflow angle for the first 40 sec of the flight. Free-stream crossflow was obtained from the taller rake, whose side ports were outside the boundary layer. Crossflow near the wall was obtained from the side ports of the shorter rake. In order to see the correlation between vehicle angle of attack and indicated crossflow angle, the regression equation for indicated crossflow near the wall as a function of angle of attack is plotted.

Pressure Distributions

Figure 20 shows three pressure distributions around the wing leading edge from the first 25 sec of the flight. Pressure coefficient is plotted against distance from the leading edge, with positive distances representing the top of the vehicle. For this plot, absolute pressure is the reference pressure used in computing the pressure coefficient. Time for the three curves are 5, 15, and 25 sec following drop, respectively. Mach numbers are 0.9, 1.3, and 1.95, respectively. And angle of attack is 14°, 18°, and 11°, respectively. The pressure distributions are smooth, which is important for judging the data.

Vibrations

Figure 21 illustrates the drop transient response from an AC-coupled accelerometer measuring the vertical component and confirms the mode existing around 12 Hz. The effects of this mode needs to be considered, because the averaging time for most of the data corresponds to 10 Hz.

Staging

The instrumentation worked up to staging (time = 95 sec, approximately) and for most sensors more than 30 sec longer. It was evident that during staging the plume from Stage 2 blasted the glove, causing an immediate jump in temperature. For example, the temperature of one of the inboard fairing tiles increased as much as 800–1000 °F in approximately 1 sec before Stage 2 had moved far enough away.

Conclusions

This paper outlined the characteristics of a transition flight experiment for transition code validation at hypersonic speeds. Performing the experiment as a secondary payload (piggyback) on a Pegasus® launch put severe requirements on the experiment. The design and fabrication of the glove, with its fairing, required unconventional solutions and extensive testing. Onboard signal processing and signal sample throughput were critical for the value of the experiment.

The severe requirements also constrained the approach taken to designing and integrating the measurement system. It was necessary to use a stepwise approach; that is, it was necessary to verify the functionality of sensors and data acquisition and processing systems in separate tests. Moreover, multiple sensing and signal processing methods were used in order to establish data validity and to minimize the impact of sensor or signal conditioning failure. From an operational perspective, the real-time display system and decision-tree analysis turned out to be invaluable for real-time assessment of go/no-go issues.

Even though the flight hardware had been manufactured and mounted on a Pegasus® wing more than one year before the experiment was manifested, the data quality and consistency was fully adequate, and valuable data was obtained for a longer time period than anticipated.

References

[1]Bertelrud, Arild, Paul Kolodziej, Gregory K. Noffz, and Afzal Godil, "Plans for In-Flight Measurement of Hypersonic Crossflow Transition on the Pegasus® Launch Vehicle," AIAA-92-4104, 6th AIAA Biennial Flight Test Conference, Hilton Head Island, South Carolina, August 24–26, 1992.

[2]Bertelrud, Arild, Geva de la Tova, Gerald B. Budd, Gregory K. Noffz, W. Lance Richards, and Richard C. Monaghan, "Pegasus® Wing-Glove Experiment to Document Crossflow Transition—Development and Current Status," AIAA 98-1522, 8th AIAA International Space Planes and Hypersonic Systems and Technologies Conference, Norfolk, Virginia, April 27–30, 1998.

[3]Saric, William S., Jon A. Hoos, and Ronald H. Radeztsky, "Boundary Layer Receptivity of Sound with Roughness," proceedings of the Boundary Layer Stability and Transition to Turbulence Symposium, 1st ASME/JSME Fluids Engineering Conference, Portland, Oregon, June 23–27, 1991.

[4]Bushnell, Dennis M. and Eli Reshotko, "Proceedings of NASP High-Speed Roughness/Waviness-Transition Interaction Workshop," NASP Workshop Publication 1005, January 1989.

[5]Mosier, Marty, Gary Harris, Bob Richards, Dan Rovner, and Brent Carroll, "Pegasus® First Mission Flight Results," 4th AIAA Utah State University Conference on Small Satellites, Logan, Utah, August 27–30, 1990.

[6]Godil, A. and A. Bertelrud, "Design of a Wing Shape for Study of Hypersonic Crossflow Transition in Flight," presented at the Symposium on High-Performance Computing for Flight Vehicles, Washington, D.C., December 7–9, 1992.

[7]Gong, Leslie and W. Lance Richards, *Thermal Analysis of a Metallic Wing Glove for a Mach-8 Boundary-Layer Experiment*, NASA/TM-1998-206555, June 1998.

[8]Richards, W. Lance and Richard C. Monaghan, "Development of a Flight Article for a Hypersonic Boundary-Layer Experiment," *AIAA Journal of Spacecraft and Rockets*, vol. 34, no. 5, pp. 609–613, September–October 1997.

[9]Horn, Thomas J. and W. Lance Richards, "Transient Thermal Testing of a Flight Test Article for High Speed Flight," 1996 World Aviation Congress, Los Angeles, California, October 21–24, 1996.

[10]Horn, Thomas J., W. Lance Richards, and Leslie Gong, *A Technique for Transient Thermal Testing of Thick Structures*, NASA TM-4803, July 1997.

[11]Howard, F. G., *Single-Thermocouple Method for Determining Heat Flux to a Thermally Thick Wall*, NASA TN D-4737, September 1968.

[12]Wright, Robert L. and Ernest V. Zoby, "Comparison of Thermal Techniques for Determining Boundary-Layer Transition in Flight," *AIAA Journal*, vol. 15, no. 11, November 1977, pp. 1543–1544.

[13]Beck, James V., Ben Blackwell, Charles R. St. Clair, Jr., *Inverse Heat Conduction: Ill-posed Problems*, John Wiley & Sons, Inc., 1985, pp. 13–15.

[14]East, L. F., "Measurement of Skin Friction at Low Subsonic Speeds by the Razor-Blade Technique," Aeronautical Research Council, London, United Kingdom, August 1966.

[15]Preston, J. H., "The Determination of Turbulent Skin Friction by Means of Pitot Tubes," *J. of the Royal Aeronautical Society*, February 1954, pp. 109–121.

[16]Keener, Earl R. and Edward J. Hopkins, *Accuracy of Pitot-Pressure Rakes For Turbulent Boundary-Layer Measurements in Supersonic Flow*, NASA TN D-6229, March 1971.

[17]Ames Research Staff, *Equations, Tables, and Charts for Compressible Flow*, NACA Report 1135, 1953.

[18]Bertelrud, Arild, Sharon Graves, John Diamond, "Development of a System for Transition Characterization," AIAA-93-3465-CP, 11th AIAA Applied Aerodynamics Conference, Monterey, California, August 1993.

[19]Bertelrud, Arild, James E. Bartlett, Harry R. Chiles, and Ronald Young, "Use of Dual Hot Films for the Measurement of Surface Mean Flow and Turbulence at High Temperatures," 41st Instrumentation Society of America Symposium, Denver, Colorado, May 7–11, 1995.

[20]Chiles, Harry R., *The Design and Use of a Temperature-Compensated Hot-Film Anemometer System for Boundary-Layer Flow Transition Detection on Supersonic Aircraft*, NASA TM 100421, May 1988.

[21]Dougherty, N. S. Jr. and David F. Fisher, "Boundary Layer Transition on a 10-Degree Cone: Wind Tunnel/Flight Data Correlation," AIAA Paper 80-0154, 1980, AIAA 18th Aerospace Sciences Meeting, Pasadena, California, January 14–16, 1980.

[22]Graves, Sharon, Arild Bertelrud, John Diamond, and Wendy Nagurny, "High Frequency Data Acquisition Using Digital Signal Processing," AIAA Paper 94-2134, 7th Biennial AIAA Flight Test Conference, Colorado Springs, Colorado, June 20–23, 1994.

[23]Hamory, Philip J., John K. Diamond, and Arild Bertelrud, *Design and Calibration of an Airborne Multichannel Swept-Tuned Spectrum Analyzer*, NASA/TM-1999-206584, October 1999.

[24]Bertelrud, A., S. Graves, R. Young, and B. Anderson, "Documentation of Crossflow Transition in Flight at Hypersonic Mach Numbers." AIAA Paper 95-6060, 6th International Aerospace Planes and Hypersonic Conference, Chattanooga, Tennessee, April 3–7, 1995.

[25]Tennekes, H. and J. L. Lumley, A First Course in Turbulence, MIT Press Cambridge, Massachusetts, September 1973.
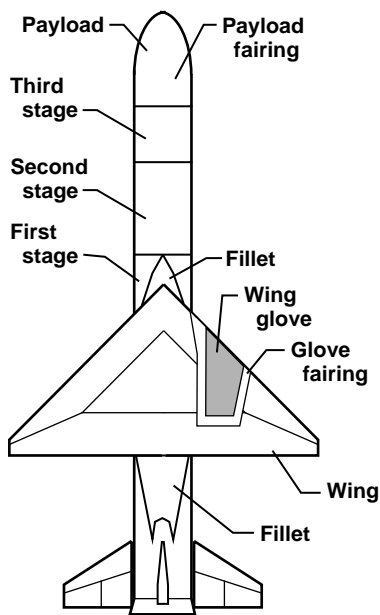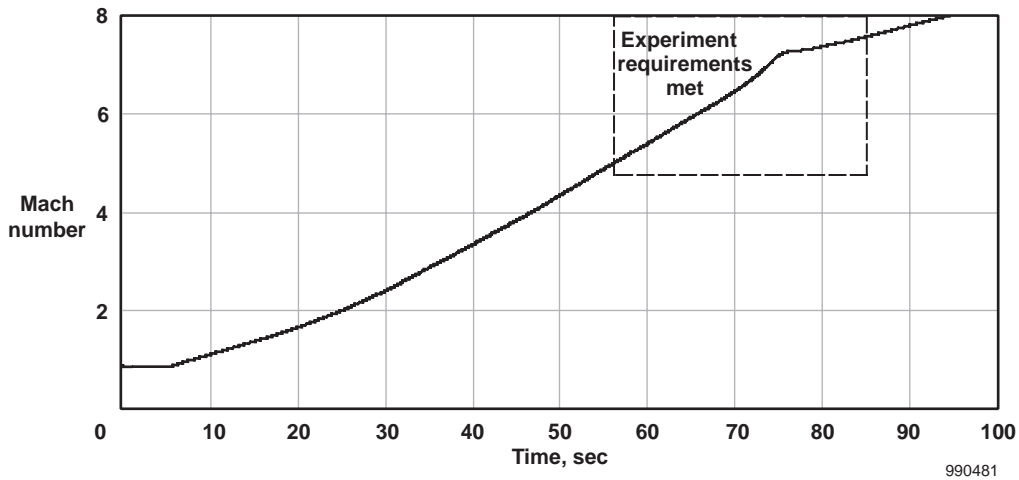
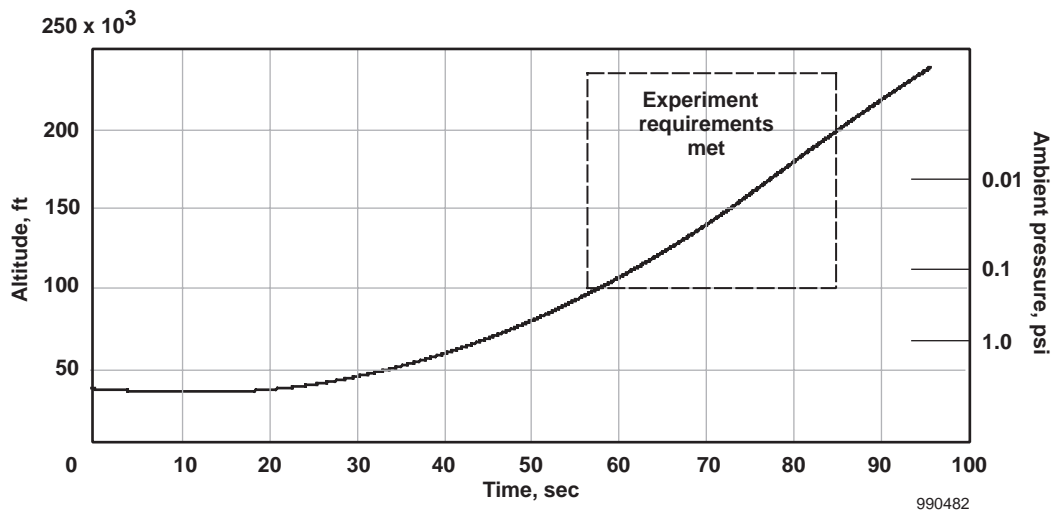Figure 1. Planform and layout of the baseline Pegasus® launch vehicle with the wing glove.
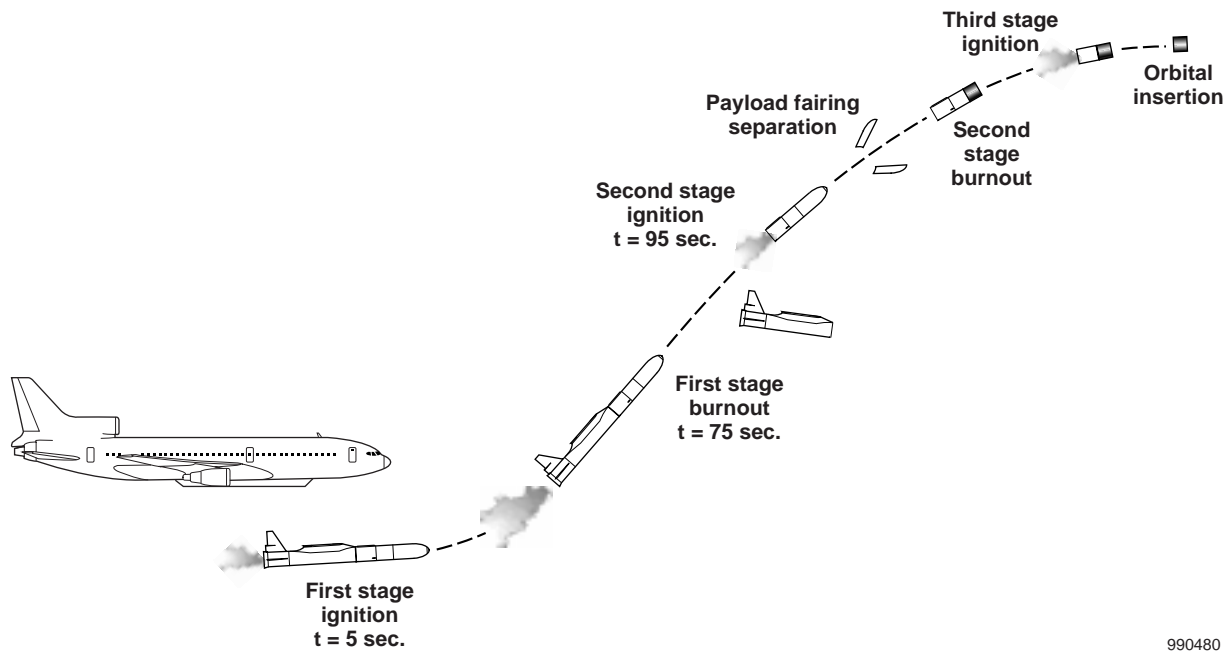
Figure 2. Illustration of Pegasus® launch events.

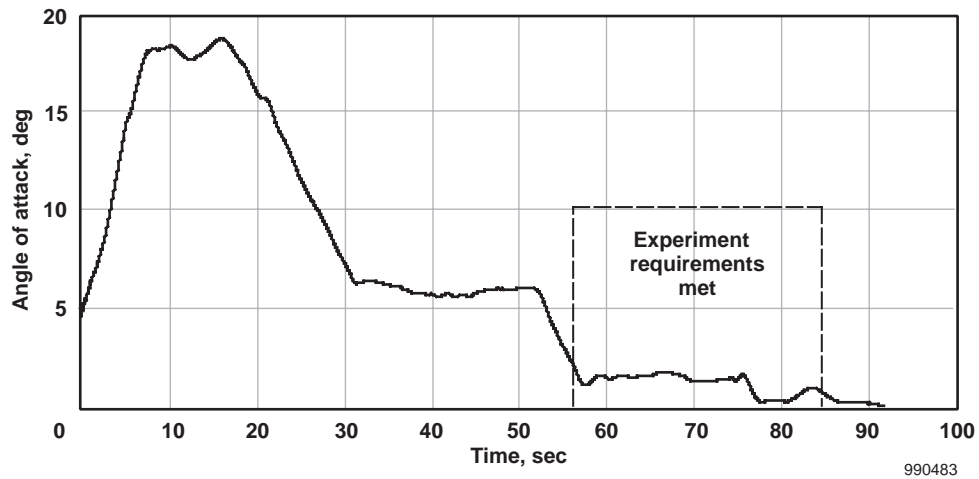(a) Mach number.

(b) Altitude.

Figure 3. Pegasus® trajectory as a function of time for launch vehicle containing FX-1.

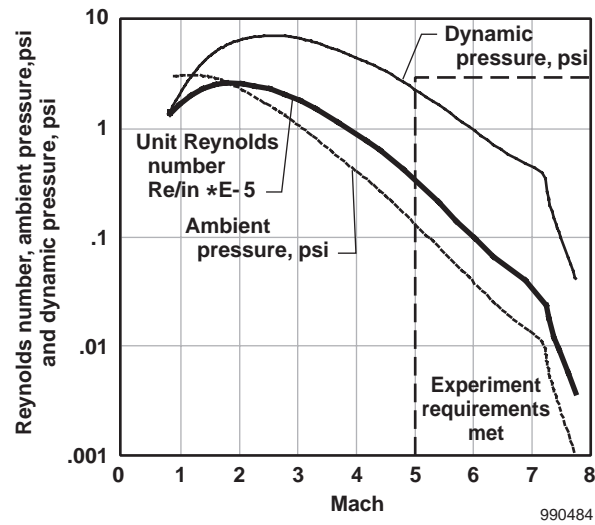American Institute of Aeronautics and Astronautics

(c) Angle of attack.

Figure 3. Concluded.

Figure 4. FX-1 trajectory represented by unit Reynolds number and ambient and dynamic pressures as a function of Mach number.

Figure 5. Photograph of glove and wing before vehicle assembly.

Fixed at inboard leading edge

See fig. 7

Ablative-coated fairing

4.27 ft (1.3 m)

Steel skin over wood support

Tile fairing

990485
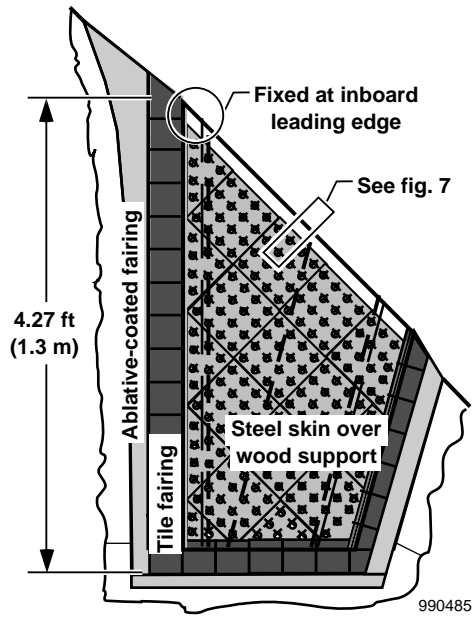
Figure 6. Plan view of glove and fairings.

Steel skin

3 mm machine screw fasteners

Wood core

Machined steel leading edge

Swivel-stud assembly

Polysulfide adhesive layer

Leading-edge overwrap

Pegasus® wing

Leading-edge fitting

Wood core

980217
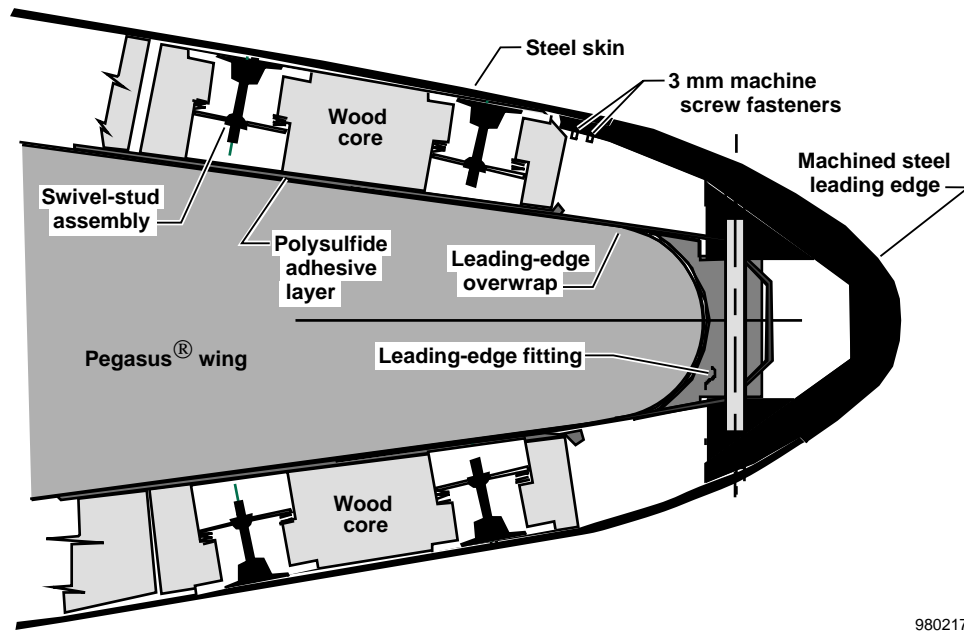
Figure 7. Cross-sectional view of leading-edge region of glove on Pegasus® wing.

American Institute of Aeronautics and Astronautics
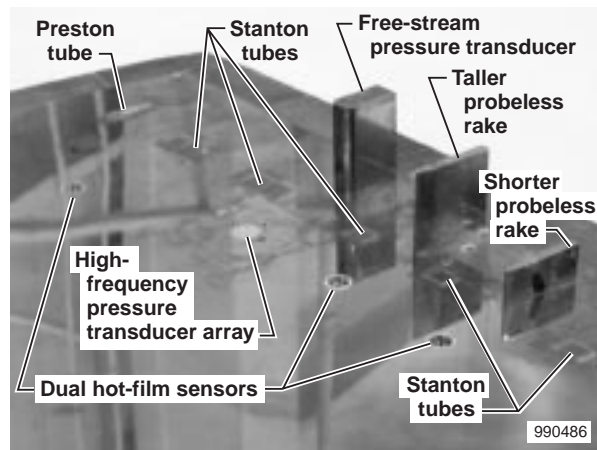
Photo by Arild Bertelrud

Figure 8. Photograph of instrumentation mounted externally toward the rear of the glove.
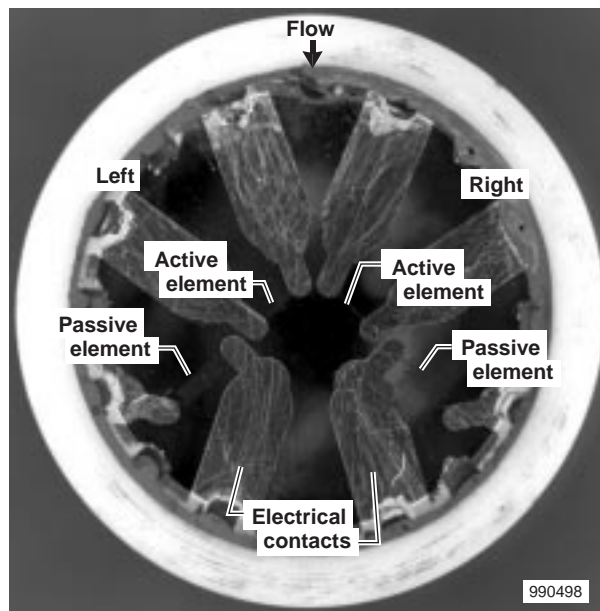
Figure 9. Photograph of dual hot-film sensor.
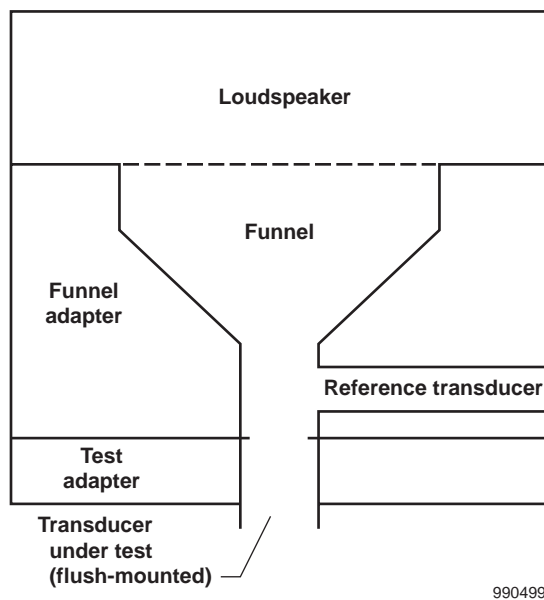
(a) Cross-sectional illustration of flush-mounted configuration.
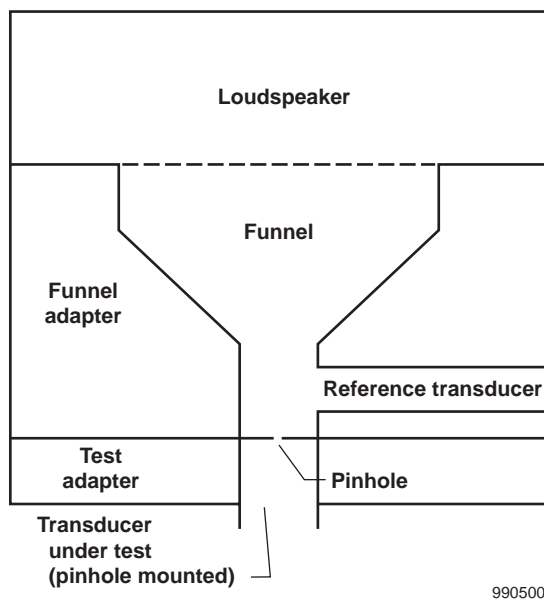
(b) Cross-sectional illustration of pinhole-mounted configuration.

Figure 10. High-frequency pressure transducer calibration apparatus.

(c) Photograph of test apparatus.

Figure 10. Concluded.
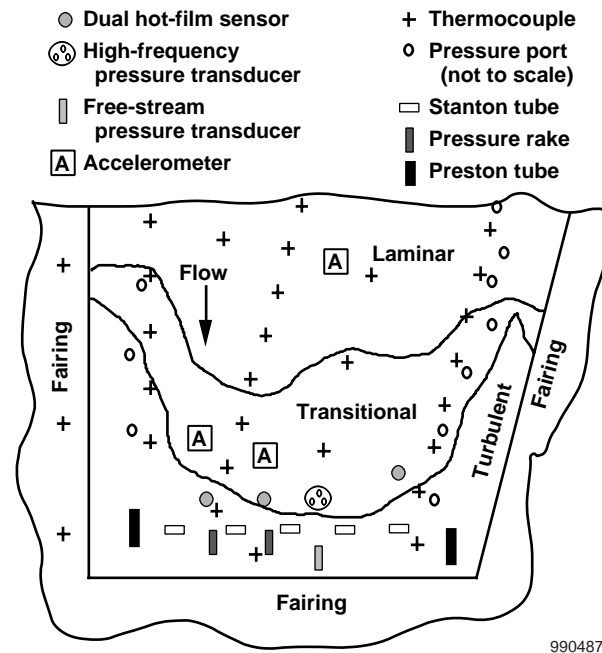
Figure 11. Sensor layout in rear part of glove with conceptual transition pattern shown.
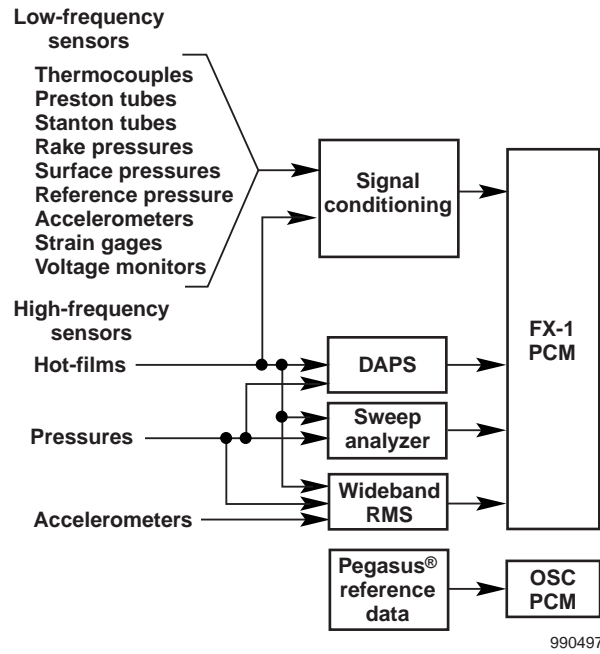
Figure 12. FX-1 Onboard instrumentation and signal processing block diagram.
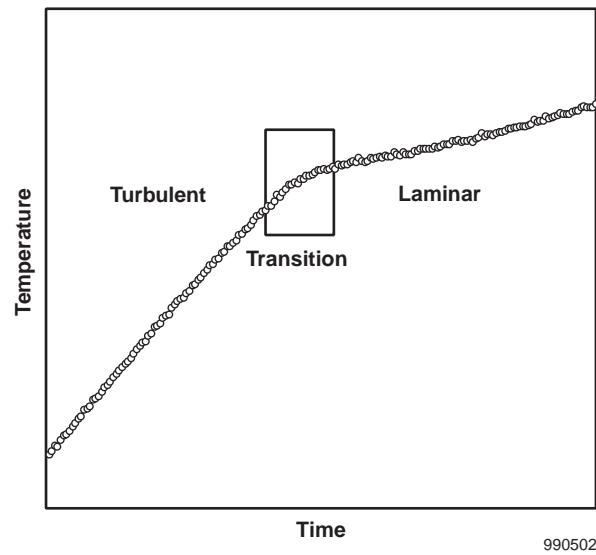
Figure 13. Time history from one thermocouple showing transition from a turbulent to a laminar boundary layer.
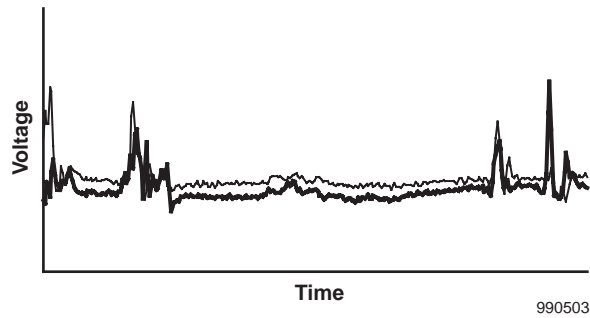
(a) Dual hot-film sensor signals.
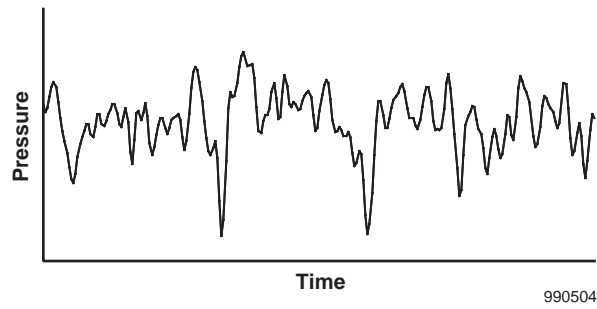
(b) Surface high-frequency pressure transducer signal.

Figure 14. Time histories for transitional flow.
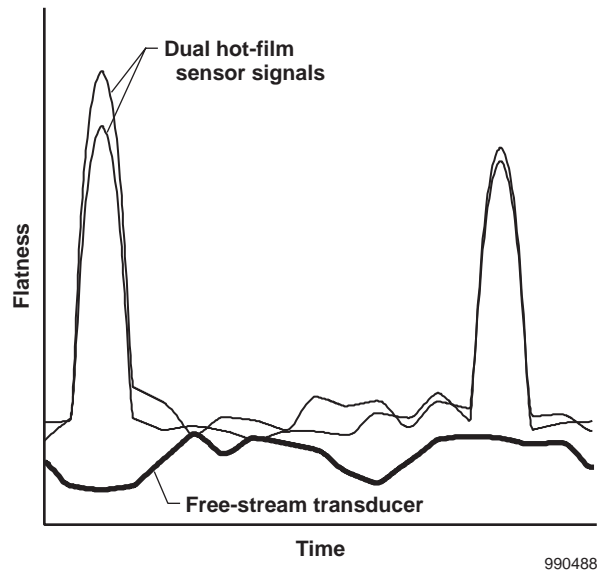
Figure 15. Flatness for the two hot-films of a dual hot-film sensor and the free-stream transducer during transition.

American Institute of Aeronautics and Astronautics
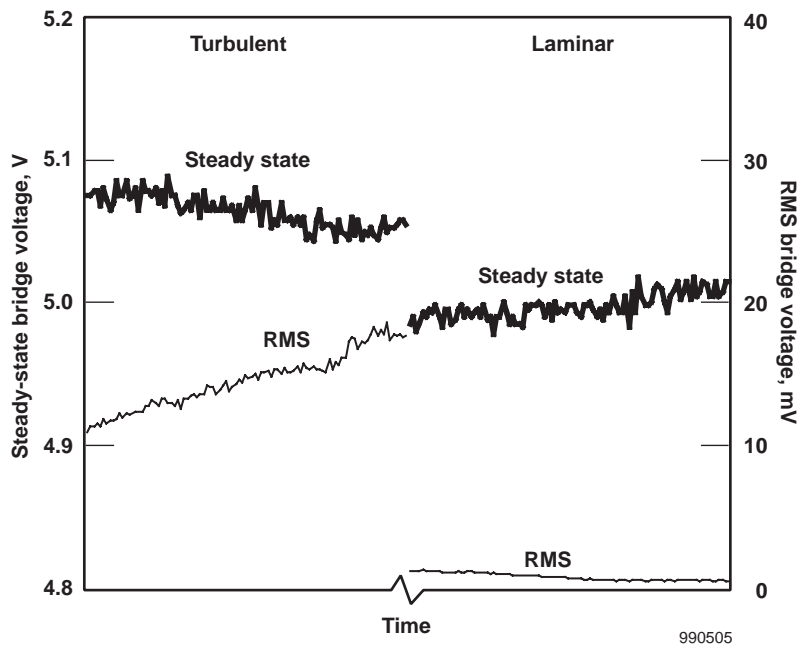
Figure 16. DC and RMS bridge voltages for one hot-film in turbulent and laminar flow.
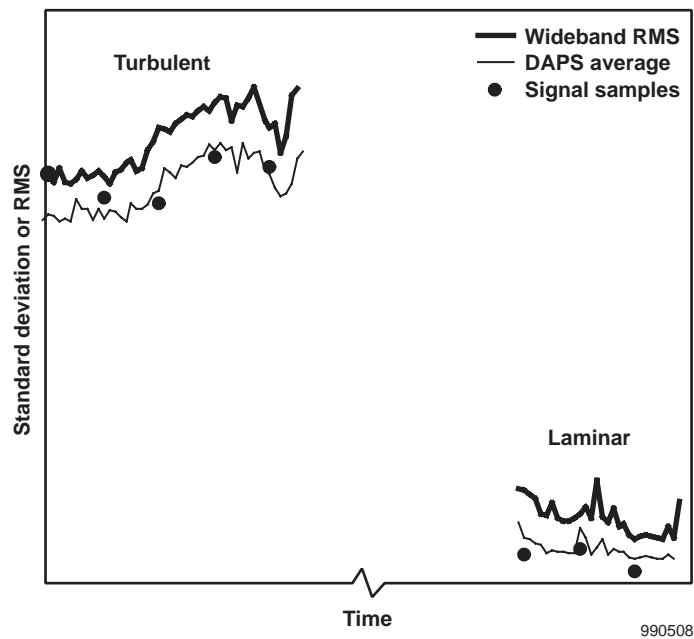
Figure 17. Turbulence results obtained with multiple processing techniques from one hot-film.

American Institute of Aeronautics and Astronautics
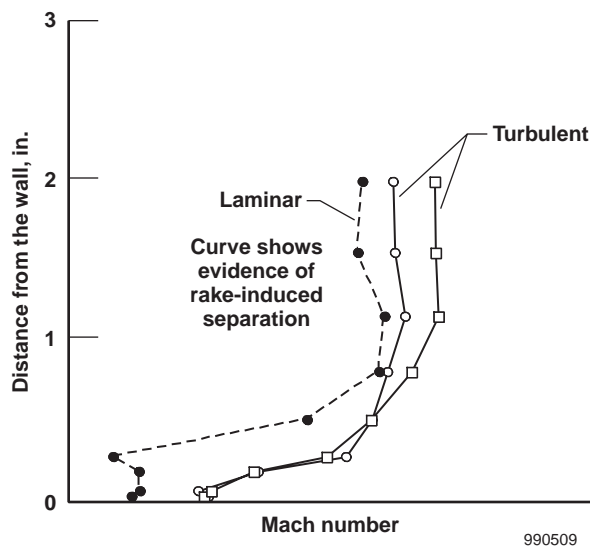
Figure 18. Total pressure distributions from the probeless rake at three points in the trajectory.
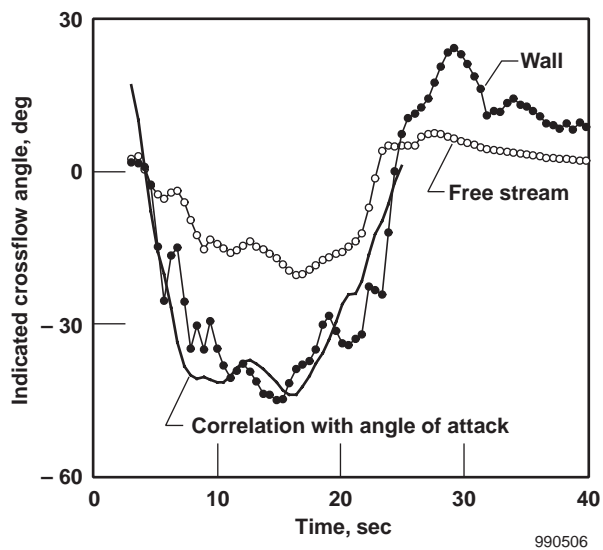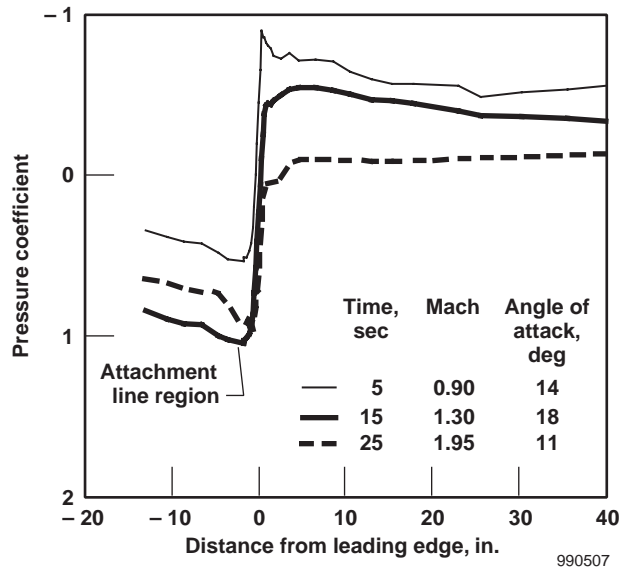

Figure 19. Crossflow angle indicated by probeless rake.

American Institute of Aeronautics and Astronautics

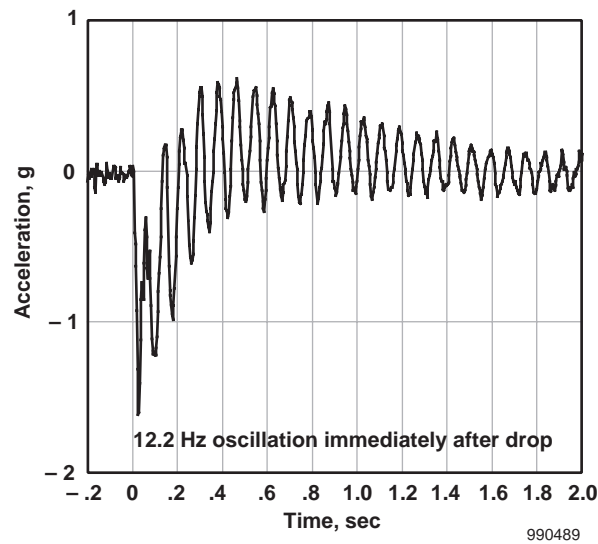Figure 20. Pressure distribution around the leading edge for three flight conditions.

Figure 21. Drop transient for the Pegasus® vehicle containing FX-1.

REPORT DOCUMENTATION PAGE

Form Approved
OMB No. 0704-0188

1. AGENCY USE ONLY (Leave blank)	2. REPORT DATE January 2000	3. REPORT TYPE AND DATES COVERED Technical Memorandum	

4. TITLE AND SUBTITLE

Pegasus® Wing-Glove Experiment to Document Hypersonic Crossflow Transition—Measurement System and Selected Flight Results

5. FUNDING NUMBERS

WU 529-55-04-E8-RR-00-000

6. AUTHOR(S)

Arild Bertelrud, Geva de la Tova, Philip J. Hamory, Ronald Young, Gregory K. Noffz, Michael Dodson, Sharon S. Graves, John K. Diamond, James E. Bartlett, Robert Noack, and David Knoblock

7. PERFORMING ORGANIZATION NAME(S) AND ADDRESS(ES)

NASA Dryden Flight Research Center
P.O. Box 273
Edwards, California 93523-0273

8. PERFORMING ORGANIZATION REPORT NUMBER

H-2395

9. SPONSORING/MONITORING AGENCY NAME(S) AND ADDRESS(ES)

National Aeronautics and Space Administration
Washington, DC 20546-0001

10. SPONSORING/MONITORING AGENCY REPORT NUMBER

NASA/TM-2000-209016

11. SUPPLEMENTARY NOTES

Presented as AIAA-2000-0505 at the 38th Aerospace Sciences Meeting and Exhibit, January 10–13, 2000, Reno, NV. A. Bertelrud, AS&M, Inc., Edwards, CA; G. de la Tova, CSC, Edwards, CA; P. J. Hamory, R. Young, G. K. Noffz and M. Dodson, NASA Dryden Flight Research Center, Edwards, CA; S. S. Graves, J. K. Diamond, and J. E. Bartlett, NASA Langley Research Center, Hampton, VA; B. Noack, WYLE Laboratories, Hampton, VA; and D. Knoblock, NASA Kennedy Space Flight Center, Cape Canaveral, FL.

12a. DISTRIBUTION/AVAILABILITY STATEMENT

Unclassified—Unlimited
Subject Category 06

12b. DISTRIBUTION CODE

13. ABSTRACT (Maximum 200 words)

In a recent flight experiment to study hypersonic crossflow transition, boundary layer characteristics were documented. A smooth steel glove was mounted on the first stage delta wing of Orbital Sciences Corporation's Pegasus® launch vehicle and was flown at speeds of up to Mach 8 and altitudes of up to 250,000 ft. The wing-glove experiment was flown as a secondary payload off the coast of Florida in October 1998. This paper describes the measurement system developed. Samples of the results obtained for different parts of the trajectory are included to show the characteristics and quality of the data. Thermocouples and pressure sensors (including Preston tubes, Stanton tubes, and a 'probeless' pressure rake showing boundary layer profiles) measured the time-averaged flow. Surface hot-films and high-frequency pressure transducers measured flow dynamics. Because the vehicle was not recoverable, it was necessary to design a system for real-time onboard processing and transmission. Onboard processing included spectral averaging. The quality and consistency of data obtained was good and met the experiment requirements.

14. SUBJECT TERMS

Boundary layer transition, Cross flow, Fault trees, Flight test instruments, Hypersonics, Onboard data processing, Pegasus air-launched booster

15. NUMBER OF PAGES

30

16. PRICE CODE

A03

17. SECURITY CLASSIFICATION OF REPORT Unclassified	18. SECURITY CLASSIFICATION OF THIS PAGE Unclassified	19. SECURITY CLASSIFICATION OF ABSTRACT Unclassified	20. LIMITATION OF ABSTRACT Unlimited